Impact of the irregular microgeometry of polyurethane foam on the macroscopic acoustic behavior predicted by a unit-cell model

O. Doutres,[1] M. Ouisse,[2] N. Atalla,[1] and M. Ichchou[3]

[1)] *GAUS, Department of Mechanical Engineering, Universite de Sherbrooke, Quebec J1K 2R1, Canada.*

[2)] *FEMTO-ST Institute, Department of Applied Mechanics, 24 rue de l'épitaphe, 25000 Besançon, France.*

[3)] *LTDS, Ecole Centrale de Lyon, 36 avenue Guy de Collongue, 69134 Ecully, France.*

(Dated: 3 September 2014)

Abstract

This paper deals with the prediction of the macroscopic sound absorption behavior of highly porous polyurethane foams using two unit-cell microstructure-based models recently developed by the authors [J. Appl. Phys. **110**, 064901 (2011) and J. Appl. Phys. **113**, 054901 (2013)]. In these models, the porous material is idealized as a packing of a tetrakaidecahedra unit-cell representative of the disordered network that constitutes the porous frame. The non-acoustic parameters involved in the classical Johnson-Champoux-Allard model (i.e., porosity, airflow resistivity, tortuosity...) are derived from characteristic properties of the unit-cell and semi-empirical relationships. A global sensitivity analysis is performed on these two models in order to investigate how the variability associated with the measured unit-cell characteristics affects the models outputs. This allows identification of the possible limitations of a unit-cell micro-macro approach due to microstructure irregularity. The sensitivity analysis mainly shows that for moderately and highly reticulated polyurethane foams, the strut length parameter is the key parameter since it greatly impacts three important non-acoustic parameters and causes large uncertainty on the sound absorption coefficient even if its measurement variability is moderate. For foams with a slight inhomogeneity and anisotropy, a micro-macro model associated to cell size measurements should be preferred.

PACS number(s): 43.55.Ev,

I. INTRODUCTION

Porous materials are heterogeneous materials composed of solid and fluid phases. According to the homogenization theory[1], the heterogeneous porous material can be considered as homogeneous if the characteristic dimensions (i.e., macroscopic wavelengths) are large compared to the size of the inhomogeneities (i.e., pore size). The wave properties at the microscopic scale can then be described according to their mean value observed at the macroscopic scale within a representative elementary volume (REV). This important consideration justifies the description of the porous media as an equivalent fluid characterized by a frequency-dependent effective density $\rho(\omega)$ accounting for inertial and viscous effects, and a frequency-dependent effective Bulk modulus $K(\omega)$ accounting for thermal effects. The well-known Johnson-Champoux-Allard (JCA) semi-phenomenological model[2–4] is used in this paper to predict the frequency behavior of the two aforementioned functions and requires the following macroscopic characteristic of the REV, also known as non-acoustic parameters: porosity ϕ, airflow resistivity σ, tortuosity α_∞, thermal characteristic length Λ' and viscous characteristic length Λ.

The JCA semi-phenomenological model is found successful to simulate the acoustical behavior of porous materials with different microstructures (e.g., foams, fibrous, granular,...). However, when used directly, this approach is not useful for microstructure optimization since by definition, it is blind to realistic microgeometrical details. To circumvent this limitation, numerous works have been proposed to link the characteristic microstructure properties to non-acoustic parameters and acoustic properties. In the particular case of acoustic foams, the three main approaches are (i) analytical[4,5] based on simplified models of the microstructure and wave propagation inside the material (also known as scaling laws)

[ref.[4]: pages 58, 68, 81 and 104], (ii) empirical[6] and semi-empirical[7,8], and (iii) numerical[9–11]. The last two aforementioned approaches (i.e., semi-empirical and numerical) are the most promising since they allow investigation of the impact of the main microstructure parameters on the wave properties without a complex description of the real microgeometry at the meso- or macro- scales and at the same time, without an excessive simplification of the idealized microgeometry. In the particular case of polyurethane acoustic foams, both approaches are based on a periodic unit-cell (called PUC) with a tetrakaidecahedral morphology representative of the complex internal structure[12,13]; the PUC is considered to be the REV in the homogenization theory. However, identifying a representative PUC of such complex and disordered 3D structure is not straightforward since most of the cells can differ from an idealized tetrakaidecahedron[13,14] and cell windows (i.e., pores) can be randomly closed or partially closed by thin membranes. Measurements of the main PUC properties can thus be subjected to an important variability related to bulk inhomogeneity, microstructural irregularities and limitations of the used measurement methods. The natural cell anisotropy can also be an important source of measurement dispersion if the PUC is defined as isotropic in the micro-macro model. The impact of the PUC variability on the estimated macroscopic acoustic properties has not been investigated in the aforementioned works. However, it is of upmost importance in order to give credit to unit-cell micro-macro approaches.

The objective of this paper is thus to investigate how the variability associated with the microstructure input characteristics of the PUC affects the macroscopic quantities (i.e, non-acoustic parameters, sound absorption coefficient) using a rigorous sensitivity analysis technique[15]. In what follows, the sensitivity analysis is applied to two semi-empirical models recently developed by the authors[7,8] to link the main microstructure properties of fully and partially reticulated polyurethane (PU) foams to the macroscopic non-acoustic parameters

involved in the JCA model. In both models, the PUC shape is an isotropic tetrakaidecahedron having struts of triangular concave cross-section shape. In the first model[7], called the 3-parameter model, the PUC is characterized by the strut length l, the strut thickness t and the reticulation rate R_w (i.e., open pore content). In the second model[8], called the 2-parameter model, the PUC is characterized by the cell size C_s and reticulation rate R_w assuming that the geometric ratio between strut length l and strut thickness t is known. It is a simplification of the 3-parameter model as the cell size is easier to characterize compared to strut's dimensions and it is also a parameter commonly used by chemists.

The sensitivity analysis is based on the Fourier Amplitude Sensitivity Test (FAST)[16–18]. FAST is a global sensitivity analysis method based on a variance decomposition which provides information about sensitivity covering the whole design space and can deal with interactions effects between input parameters. It is an efficient technique that allows estimation of the "main effect" (also named first order term) and the so-called "Total Sensitivity Indexes" (TSI)[15]. The sensitivity analysis is split in two parts in order to clearly differentiate the contribution of (i) the model sensitivity and (ii) the variability of the PUC properties. First, the sensitivity analysis is applied to three virtual foams for which all microstructure characteristic parameters of the PUC share the same variability (i.e., 10 % of the nominal value). This allows identification of the input parameters contributing the most to output variability. These parameters thus require precise measurement and/or to be barely affected by PUC variability (bulk inhomogeneity, irregularity, natural cell anisotropy) in order for the unit-cell model to give reliable estimation of the macroscopic acoustical behavior. The sensitivity analysis method is then applied to real foams already investigated in refs.[7,8] to account for the real input variability and weight the conclusions drawn for virtual foams.

This paper is organized as follows. In Sec. II, the complex microgeometry of polyurethane

foams and the microstructure characterization procedure are detailed. The porous modeling and the micro-macro relationships are then briefly recalled. Sec. III presents the main principles of the sensitivity analysis method. Sec. IV applies the FAST method to virtual foams with controlled microstructure variability and then to real PU foams for which the microstructure has been characterized directly from micrographs. Sec. V uses the conclusions derived from the sensitivity analysis in order to investigate the relevance of using a microstructure-based model in an inverse approach to assess equivalent microstructure properties. The conclusions of this work are presented in Sec. VI.

II. MICROSTRUCTURE BASED MODELING

A. Foam microgeometry and characterization

Polymeric foams produced at a large scale industrial process can be classified in two categories, according to the amount of material property variability which is observed in the manufactured product. The first category is characterized by "low variability" foams manufactured in large volumes and which properties are relatively tightly controlled. Such foams are used for example as acoustic treatments for buildings, cars or planes and also as cores for composite structures. The second category is composed of highly variable foams that are produced in small batches. For example, foam components with complicated shapes such as car seats are produced by injection molding which creates impervious skins on top of the foam component surfaces and thus leads to large microstructure inhomogeneity within the foam volume. For both categories, the produced foams are anisotropic due to the

preferential evolution of the foam in the rise direction during the foaming process.

The class of flexible polyurethane foams considered in this paper and in previous works[7,8] belongs to the first category of low variability foams. These foams have been produced initially in very large volume and then sliced to 1 in. or 2 in. thick boards. The microstructure of the foams is made of a 3D network of interconnecting struts made of polyurethane resin, the struts being integrally interconnected by thickened nexi to form a skeleton including polyhedrons with polygonal faces (see Fig. 1). The foam microgeometry was found to be in general disordered, consisting of a variety of cell shapes[13] but the tetrakaidecahedral cell (also known as *Kelvin cell*) characterized by an average of 14 faces (i.e., windows) per cell and 5.1 edges (i.e., struts) per face is found to be the most satisfying approximation of the mean cell shape. Furthermore, as mentioned by Zhu *et al.*[12], the tetrakaidecahedron is the only polyhedron that packs with identical units to fill space and which nearly satisfies the minimum surface energy conditions. Thin membranes of polyurethane, bridging between the struts of the skeleton and closing the polygonal faces are created during the foaming process[19]. The membrane opening is roughly controlled and the open pores or partially open pores are randomly distributed within the irregular cell arrangement. Materials having only open pores are called fully reticulated, while if some of the pores are closed or partially closed, the material is partially reticulated. The PU foams considered in this work are light and highly porous: the frame density ρ_1 is ranging between 21.5 kg.m^{-3} and 29 kg.m^{-3} and the open-porosity ϕ is ranging between 96.8 % and 99 %. The foaming process was controlled to modify the cell size and the amount of closed pores while keeping the porosity and the frame density in the aforementioned range of variation. By controlling these two microstructure parameters it is possible to create PU foams with an airflow resistivity σ varying from 100 N.s.m^{-4} to 150000 N.s.m^{-4}. This class of material is thus very interesting

since it allows coverage of most of the acoustical behaviors usually encountered for sound insulation or sound absorption applications.

The two semi-empirical micro-macro models developed for the class of PU foams[7,8] described previously idealize the porous microstructure as a packing of isotropic tetrakaidecahedral PUC as shown in Fig. 1(d) [note that this idealized structure is possible since all foams own to the first category of "low variability" foams in an industrial point of view]. The struts of the PUC have a triangular concave cross-section shape which is considered constant along the strut length and the accumulation of material at the nodes is neglected. The properties of the representative PUC are: cell size C_s [μm], strut length l [μm] and thickness t [μm], reticulation rate R_w [%]. All these properties are measured from 2D SEM-micrographs using the "ImageJ" software[20]. The microtomography technique associated to an automatic characterization procedure cannot be used for flexible PU foams since it is not able to properly captures the thin pores' membranes. The PUC characterization is thus carried out manually which may add variability depending on the experimenter. However, for this complex and inhomogeneous microgeometry as shown in figure 1, it is considered that the variability brought by the experimenter is negligible compared to the one due to the microgeometry irregularity.

FIG. 1.

In order to grasp the effect of the natural cell anisotropy, the microstructure properties measurements are carried out on pictures taken in the plane parallel to the wave propagation and in the plane perpendicular to the acoustic wave propagation. The cell size C_s is first measured with great care since only cells that have been cut at the middle must be considered (see Fig. 1(a)). The Degree of Anisotropy of the cell (DA), defined as the large to small cell radius ratio, is estimated for both planes and the highest value is stored. All foams

with $DA > 1.25$ were rejected from the analysis in order to work only with "quasi-isotropic" PU foams and be consistent with the isotropic tetrakaidecahedral PUC. Quasi-isotropic PU foams can be defined as foams for which the natural anisotropy observed at the micro-scale has no significant impact at both the meso- and macro- scales. In this case, the classical JCA model can be used with scalar non-acoustic inputs and not tensors as required for highly anisotropic foams[21]. Furthermore, acousticians and/or chemists would prefer to use isotropic material models (even for slightly anisotropic foams) in order to predict the acoustical behavior of foams because the number of experimental tests to identify parameters is much less time-consuming, specially, during the conceptual and preliminary design phases. The sensitivity analysis proposed in this work will thus provide a framework, indicating the impact of applying such isotropic micro-macro models to real foams for which the input variability will be clearly affected by the natural anisotropy.

The struts of polyurethane foams have a triangular concave cross-section shape. The area of the cross-section is not constant along strut length[13]: it is maximum at the two ends because of the accumulation of material at the nodes and is minimum at the center. The geometry of the PUC strut is simplified and the area of the cross-section is considered constant along strut length. Only the edge a of the triangle is measured on the micrographs (see Figs. 1(b) and 1(d)) and it is always measured in the middle of strut length. The strut thickness t is the height of this triangle assumed equilateral and is thus given by $t = a\sqrt{3}/2$.

Quasi-isotropic PU foams are idealized from isotropic tetrakaidecahedral PUC with interconnected struts of equal length: $l_1 = l_2 = l_3$ (see Fig. 1(d)). However, a large difference is observed between these three characteristic dimensions in the case of real PU foams as shown in Fig. 1(a)-1(c). The strut length l is thus derived as the mean value from the three dimensions l_1, l_2, and l_3; procedure which is repeated multiple times within the micrographs.

Characterizing the mean strut length from this procedure allows better identification of this property compared to an average of individual struts chosen arbitrarily within the micrographs. Indeed, it has been observed that the later method often overestimates the strut length parameter since it gives artificially more weight to longer struts. It is clear that large differences between l_1, l_2 and l_3 may be observed on anisotropic foams (see Fig. 1). However, this large difference may also be observed on quasi-isotropic foam (characterized by an isotropic tetrakaidecahedra PUC) for which the hexagonal pores are much larger than the squared pores. Thus, a large variability measured for l should not always be interpreted as an indication of cell anisotropy.

The reticulation rate R_w [%], which gives the open window content of the material, is estimated by the ratio of the number of visible open windows to the total number of windows visible on the pictures. An example is given in Fig. 1(d). Most of the time, the distinction is clear between the two kinds of pores. However, when present, the half open pores were considered open. This measurement method is in good agreement with the one used by Zhang et al.[22]. Note that the optical microscopy is unable to capture all the open and closed pores due to its very short depth of field and and R_w can only be assessed from SEM micrographs. The reticulation rate is neither defined nor measured at the cell scale but rather at a meso-scale since numerous cells with closed and open pores are present on the micrographs. The parameter variability is still assessed since measurements are carried out on multiple micrographs taken at different locations on the foam board surface.

In order to ensure that the characterized unit-cell is representative of a mean cell for each material, all properties and associated expanded uncertainties are determined from a large number of measurements: e.g., 20 measurements for C_s, t, and l, and approximately 800 windows analyses to estimate R_w. Even if these microstructure properties are measured

using sophisticated optical methods (i.e., SEM), a large variability can be observed due to the great complexity of the 3D microstructure and the precision of the measurement device and method. Another measurement bias is related to the evaluation of the dimensions of 3D struts (t and l) from 2D pictures. However, the systematic errors induced by this procedure can hardly be quantified. The levels of variability will be described when used in the paper.

B. Porous material model

According to the JCA model[2–4], the two dynamic properties $\rho(\omega)$ and $K(\omega)$ of the equivalent fluid are derived from their low to high-frequency asymptotic behaviors using specific viscous and thermal dynamic tortuosity functions, $\alpha(\omega)$ and $\alpha'(\omega)$, such as

$$\rho(\omega) = \rho_0 \alpha(\omega), \tag{1}$$

$$K(\omega) = \frac{P_0}{1 - \dfrac{\gamma - 1}{\gamma} \alpha'(\omega)^{-1}} \tag{2}$$

with

$$\alpha(\omega) = \alpha_\infty + \frac{\phi\sigma}{j\omega\rho_0} \left[1 + \left(\frac{2\alpha_\infty \eta}{\Lambda^2 \phi \sigma} \right) \frac{j\omega}{\nu} \right]^{1/2}, \tag{3}$$

$$\alpha'(\omega) = \left(\frac{8\nu'}{j\omega\Lambda'^2} \left[1 + \left(\frac{\Lambda'}{4} \right)^2 \frac{j\omega}{\nu'} \right]^{1/2} + 1 \right), \tag{4}$$

where ω is the angular frequency, ρ_0 is the fluid density, η is the fluid viscosity, $\nu = \eta/\rho_0 = P_r \nu'$ is the kinematic fluid viscosity, P_r the Prandtl number, P_0 the atmospheric pressure, and γ the specific heat ratio.

The macroscopic non-acoustic parameters ϕ, σ, α_∞, Λ and Λ' used to describe the visco-inertial and thermal couplings between the porous aggregate and the interstitial fluid will

be defined in the following subsection. In particular, Eqs. (1) and (3) describe the visco-inertial interactions between the two phases. At low frequencies, the viscous forces dominate whereas at high frequencies the behavior is governed by inertial forces. The viscous/inertial transition frequency f_v can be approximated by $f_v = \phi\sigma/(2\pi\rho_0\alpha_\infty)$ (see ref.[4], chap. 5.10.2 page 96). The real part of the dynamic bulk modulus (from Eqs. (2) and (4)) describes an isothermal process at low frequencies (its value approaches asymptotically unity)[3] and an adiabatic process at high frequencies (its value approaches 1.4). The imaginary part related to thermal dissipation is close to zero at both low and high frequencies and reaches a maximum at the transition frequencies between isothermal and adiabatic processes. The isothermal/adiabatic transition frequency f_t can be approximated by $f_t = 8\nu'/(2\pi\Lambda'^2)$. Note that the thermal dissipation is generally negligible compared to the viscous dissipation (see ref.[4], page 89).

The homogeneous foam layer is often described by the following two intrinsic acoustical properties: the wave number $k(\omega) = \omega\sqrt{\rho(\omega)/K(\omega)}$ and the characteristic impedance $Z_c(\omega) = \sqrt{\rho(\omega)K(\omega)}$. The acoustic performance indicators of interest in this paper are the impedance at normal incidence when the equivalent fluid layer of thickness H is backed by an impervious rigid wall, namely

$$Z_s(\omega) = -jZ_c(\omega)\cot(k(\omega)H)/\phi \tag{5}$$

and the normal incidence sound absorption $\alpha(\omega)$ which is derived from the reflection coefficient r such as

$$\alpha(\omega) = 1 - |r(\omega)|^2, r = \frac{Z_s(\omega) - \rho_0 c_0}{Z_s(\omega) + \rho_0 c_0}, \tag{6}$$

c_0 being the sound speed in air.

The five non-acoustic properties of isotropic and homogeneous polyurethane open-cell foams (i.e., ϕ, σ, α_∞, Λ and Λ') are estimated from microstructure properties, i.e. cell size C_s, strut length l, strut thickness t and reticulation rate R_w, using the two semi-empirical models recalled in the two following sub-sections.

It is worth noting that the transmission loss of the PU foams could have also been computed from the two semi-empirical micro-macro models associated to the JCA model. However, only the sound absorption coefficient is investigated in this paper for conciseness.

C. The 3-parameter semi-empirical model

The 3-parameter model[7], initially developed for quasi-isotropic PU foams, considers the porous media as a packing of isotropic tetrakaidecahedra cells interconnected through pores as shown in Fig. 1. The links between microstructure and non-acoustic properties are derived using a combination of (i) geometrical calculations derived on the PUC, (ii) augmented scaling laws to account for the presence of closed pores and (iii) empirical observations. This model requires measurements of three characteristic microstructure properties of the PUC as shown in Figure 1; strut's length l [μm], strut's thickness t [μm], and reticulation rate R_w [%] (i.e., open pore content).

According to their definition, both porosity ϕ and thermal characteristic length Λ' are purely geometrical macroscopic parameters. The porosity is defined as the ratio of the fluid volume V_f to the total volume V_t in a REV that contains a sufficient number of cells but remains small at a macroscopic scale. The thermal characteristic length Λ' is the effective radius of the pores defined by Champoux and Allard[3] as twice the average ratio of the cell volume V_f to the wet surface A_t. Since the porous material is idealized as a packing of the representative unit-cell, both ϕ and Λ' are determined from simple geometrical calculations

based on the size and shape of this unit-cell. These two parameters are given by:

$$\phi = \frac{V_f}{V_t} = 1 - C_t^{\rho} \left(\frac{t}{l}\right)^2, \tag{7}$$

$$\Lambda' = \frac{2V_f}{A_t} = \frac{8l\sqrt{2}}{3} \frac{1 - \dfrac{t^2\left(2\sqrt{3}-\pi\right)}{l^2\sqrt{2}}}{1 + 2\sqrt{3} - R_w\left(1 + 2\sqrt{3} - \dfrac{4\pi t}{l\sqrt{3}}\right)}, \tag{8}$$

with V_f the fluid volume within the cell, V_t the total cell volume and A_t the surface of the frame in contact with the saturating fluid. The constant C_t^{ρ} is equal to $\left(2\sqrt{3}-\pi\right)/\sqrt{2}$ since the struts of PU foams have a triangular concave cross-section shape. As mentioned previously, the struts of the representative unit-cell are assumed to be straight, to have a triangular concave cross-section which remains constant along the strut. The void volume at the strut connections is neglected here (as shown in Fig. 1); which thus restricts the study to highly porous foams.

The airflow resistivity σ links the macroscopic fluid velocity to the imposed pressure gradient according to Darcy's law. It is particularly relevant to describe the viscous interaction between the frame and the saturating fluid at low frequencies. In the case of fully reticulated PU foams (i.e. R_w=100%), it is predicted in ref.[7] by using a scaling law that combines different simplified models of wave propagation inside the material as suggested by Lind-Nordgren and Göransson[23]. This scaling law is then generalized empirically in ref.[7] for partially reticulated foams and thus accounts for the presence of thin membranes closing the cell windows. The generalized expression is given by

$$\sigma = C^{\beta} \left(C_r^{\rho} \frac{t}{l^2}\right)^2 \left(\frac{1}{R_w}\right)^{1.1166}, \tag{9}$$

with $C_r^{\rho} = 3\pi/8\sqrt{2}$, $C^{\beta} = 128\eta$ and η the dynamic fluid viscosity taken equal to $1.85 \times$

$10^{-5} Pa.s$.

The tortuosity α_∞ is used in the models to account for the inertial interaction between the frame and the saturating fluid at high frequencies. It characterizes the dispersion of the microscopic particle velocity around the macroscopic mean value and is often interpreted as a characteristic of the sinuous aspect of the path associated with the passage of a wave in the porous media. The viscous characteristic length Λ is defined similarly to Λ' but each surface or volume components are weighted by the local particle velocity (considering an ideal fluid). Both α_∞ and Λ thus depend on the local fluid velocity in the porous aggregate. Since the complex microstructure of real PU foam prevents accurate analytical representation of the velocity field, an empirical approach is chosen in ref.[7] to estimate these two properties:

$$\Lambda = \frac{\Lambda'}{n} = \frac{\Lambda'}{1.55} \left(\frac{1}{R_w} \right)^{-0.6763}, \tag{10}$$

$$\alpha_\infty = 1.05 \left(\frac{1}{R_w} \right)^{0.3802}. \tag{11}$$

The two coefficients 1.05 and 1.55 have been determined empirically for fully reticulated PU foams and it has been shown that both n (i.e., the ratio between the thermal and viscous characteristic lengths) and α_∞ increase with the close pore content (1-R_w). Note that $n = 1.55$ found for fully reticulated foams is close to the the value of 2 determined analytically in the case of idealized highly porous fibrous materials[2–4] (ref.[4] see pages 80,81,106 and 107).

D. The 2-parameter semi-empirical model

In order to simplify the characterization of the PUC, a 2-parameter model for highly porous PU foam has been proposed in ref.[8]. The model simplification is based on the fact that the 3-parameter model has been developed for the sound absorbing class of PU foams

having a porosity ranging between 96.8% and 99% and a frame density between 21.5 kg.m^{-3} and 29 kg.m^{-3}. For this class of PU foams, the geometric ratio between strut length l and strut thickness t has been found equal to $B = l/t = 3.78 \pm 0.53$. Furthermore, by considering an isotropic tetrakaidecahedra unit-cell, the strut length l is related to the cell size C_s according to the simple geometrical relation $l = C_s/A\sqrt{2}$ with $A = 2$. The geometric ratio A has been found experimentally equal to 2.33 ± 0.36 in ref.[8] which is in accordance with the tetrakaidecahedra shape of the unit cell. This model thus requires measurements of only two microstructure properties; the cell size C_s and reticulation rate R_w. The measurement process is thus considerably simplified since strut's dimensions are no more required and the model becomes more compatible with chemists'work who commonly deal with the cell size property (the foam is usually characterized by its cell density in pore per inch [ppi] which, for the foams considered in this work, is related to the cell size considering an average of two pores per cell).

Using the two geometric factors A and B, the relations between microstructure and non-acoustic properties can be rewritten as:

$$\phi = 1 - \frac{C_t^\rho}{B^2}, \tag{12}$$

$$\Lambda' = \frac{8C_s}{3A} \frac{1 - \left(2\sqrt{3} - \pi\right)/B^2\sqrt{2}}{\left(1 + 2\sqrt{3}\right) - R_w\left(1 + 2\sqrt{3} - 4\pi/B\sqrt{3}\right)}, \tag{13}$$

$$\sigma = C^\beta \left(C_r^\rho \frac{A\sqrt{2}}{B}\right)^2 \left(\frac{1}{C_s}\right)^2 \left(\frac{1}{R_w}\right)^{1.1166}. \tag{14}$$

It is worth reminding that the 2-parameter model is dedicated, through the B parameter, to acoustic PU foams for which the porosity and frame density belongs to a specific area of validity ($96.8\% < \phi < 99\%$ and 21.5 kg.m^{-3} $< \rho_1 <$ 29 kg.m^{-3}). Considering a given PU foam, both properties should thus be estimated in a first place. The frame density ρ_1

of a foam sample is simply determined according to standard ASTM D-3574[24] test A from the ratio of the sample mass to the sample volume. If ρ_1 belongs to its area of validity, the porosity can thus be estimated from ρ_1 and the strut material density ρ_s ($\rho_s \approx 1190$ kg.m^{-3} for PU foams) using the equation proposed by Gibson and Ashby[5]: $\phi = 1 - \rho_1/\rho_s$ (it is considered that the assumptions related to this equation are valid for this class of foam). It is important to note that the porosity is not an input of the semi-empirical models and should not be measured. The 2-parameter model could be applied to other class of foams as long as it is highly porous and characterized by an idealized isotropic tetrakaidecahedra PUC. In this case, the porosity should be measured directly and the coefficient B estimated from an inverse procedure based on Eq. (12): the 2-parameter model then becomes a 3-parameter model.

III. SENSITIVITY ANALYSIS METHODS

A so-called global sensitivity analysis method is used in this work. Detailed calculations related to the method have been omitted for conciseness and clarity. For more information, the reader is referred to the following references[15–18,25–27]. A global sensitivity analysis method is able to estimate the sensitivity of a model to large variations of input parameters using a variance decomposition and identify input parameters cross coupling effects. The Fourier Amplitude Sensitivity Test (FAST) is an efficient technique that can be used to estimate the "main effect" (also named first order term) and the "Total Sensitivity Indexes" (TSI). Indeed, concerning a quantity of interest (the output of the model), the Total Sensitivity Index of parameter i, denoted by $TSI(i)$, is defined as the sum of all the sensitivity indexes (including all the interactions effects) involving parameter i. For example, suppose that we only have three input parameters, namely A, B and C in our model. The total

effect of parameter A on the output is $TSI(A) = SI(A) + SI(AB) + SI(AC) + SI(ABC)$. Here, $SI(A)$ denotes the first order sensitivity index for parameter A, $SI(AX)$ is the second order sensitivity index for the parameter A and X (for $X \neq A$), i.e. the interaction between parameters A and X, and so on. The first order sensitivity index does not take into account coupling effects between parameters, but considers variation of the parameter according to its statistical distribution on a possibly large range. All indexes can be estimated using variance decomposition methods, which are most of the time based on random samplings. The FAST technique uses Fourier transforms associated to specific sampling strategy to estimate the sensitivity indexes. The indexes presented here are normalized to unit, and are presented together with the "Normalized Standard Deviation" (NSD) of the output of interest. Indeed, the use of normalized indexes allows efficient ranking of parameters, but the variance level should not be forgotten during the analysis of the results. For proper analysis of the sensitivity issues, each time that SI or TSI indexes are presented, we will also give the value of the normalized standard deviation

$$NSD(y) = \frac{\sqrt{E(y^2) - E(y)^2}}{E(y)} \tag{15}$$

as a measure of the level of variability of the feature of interest. Note that the sensitivity analysis method could hardly be applied to a unit-cell micro-macro model based on numerical approach due to the large associated computation cost (the sensitivity analysis requires a great number of random combinations for convergence).

IV. IMPACT OF THE "PUC" VARIABILITY

The objective of this work is to show how the macroscopic acoustic properties of PU foams are impacted by the PUC variability. Before going into the details of the analysis, it should be emphasized that the sensitivity analysis results of real foams must be interpreted regarding the knowledge of inputs, which includes geometrical irregularities effects in the foams (i.e., effect of cell anisotropy, inhomogeneity within the bulk volume), together with uncertainties due to measurement procedures. In particular, it should be understood that a parameter could be classified as almost insensitive due to the fact that (i) it has been identified in a very precise manner experimentally, (ii) this parameter is barely affected by bulk inhomogeneities or (iii) simply because the model is not much sensitive to this parameter. The following analysis is thus split in two parts. First, the sensitivity analysis is applied to virtual foams for which all microstucture characteristic parameters of the PUC share the same variability (i.e., 10 % of the nominal value). This allows identification of the input parameters contributing the most to output variability, thus requiring (i) precise measurement and/or (ii) to be barely affected by bulk inhomogeneity and natural cell anisotropy. The method is then applied to real foams already investigated in refs.[7,8] to account for the real input variability and weight the conclusions drawn for virtual foams. The calculations and measurements presented here correspond to a material thickness of 2 in., except for materials P1, P2 and P3, which are 1 in. thick. This choice will be discussed later.

A. Focus on sensitivity analysis on virtual foams

The three virtual polyurethane foams with nominal microstructure properties given in Table I are considered: material V1 has small cells and is highly reticulated, material V2

has small cells and is poorly reticulated and material V3 has large cells and is moderately reticulated. All non-acoustic properties and transition frequencies f_v and f_t of the materials were calculated from C_s and R_w according to Sec. II and are given in Table II. Note that in the case of the 3-parameter model, the nominal strut dimensions l and t are calculated from the nominal cell size C_s given in Table I and the two geometric ratios A and B (the 2 micro-macro models thus provide the same non-acoustic parameters). All virtual materials are 2 in. thick.

In the proposed sensitivity analysis, the variability of the microstructure inputs is set to 10 % of the nominal value (see Table I). The value of 10 % has been chosen from experimental observations and is identical for all inputs. As mentioned previously, considering identical variability allows estimation of the inputs contributing the most to the output variability without taking into account the real sources of the variability; i.e., effect of natural cell anisotropy, inhomogeneity within the bulk volume and measurement bias. Indeed, these variability contributions are different for each microstructure input and will affect the conclusions of the sensitivity analysis. The minimum and maximum of each input for the three virtual materials are given in Table I. The probability density functions are chosen uniform for all inputs. In the case of the 3-parameter model, the nominal strut dimensions l and t are calculated from the nominal cell size C_s given in Table I and the two geometric ratios A and B. The variability of l and t is then set to 10 % of their nominal value.

The results of the sensitivity analysis for the three virtual foams V1, V2 and V3 and considering the 3-parameter semi-empirical model are given in Figs. 2. Figures 2(a), 2(c) and 2(e) show the NSD of the five non-acoustic parameters and their first order sensitivity index SI to input parameters l, t and R_w. As mentioned previously, the NSD criterion gives information about the global variability of the output. It is presented in the histogram

as the total height of the vertical bars. This criterion allows weighting of the conclusions that are drawn from the sensitivity indexes[27]. Only the first order sensitivity indexes SI are presented in the figures since it has been observed that the couplings between microstructure parameters were negligible (i.e., $TSIs \approx SIs$). This is a pertinent trend for the model since it indicates that optimizations can be performed on individual parameters to improve the efficiency of the material without any risk related to unexpected coupling effects. In order to simplify the sensitivity analysis and ease the figures readability, the SI of the three microstructure inputs of each non-acoustic output are normalized and plotted together within the NSD bar.

In the case of the highly reticulated foam V1 ($R_w = 80$ %), Fig. 2(a) shows that the variability of ϕ and α_∞ is insignificant. The geometrical model developed for porosity (see Eq.(7)) is dedicated to highly porous materials and is little sensitive to small variation of strut dimensions. This would be verified for all foams investigated in this paper. Furthermore, the tortuosity α_∞ has been shown in ref.[7] to depend only on the reticulation rate R_w (see Eq.(11)). The impact of R_w is low in this case ($NSD < 5\%$) since foam V1 contains very little membranes. Fig. 2(a) also shows that the variability of σ, Λ and Λ' is moderate ($NSD < 30$ %); the airflow resistivity σ is the most impacted parameter. The strut length variability is mainly responsible for the observed outputs sensitivity (see green surface): it captures around 80 % of the airflow resistivity σ and thermal characteristic length Λ' sensitivity. On the contrary, the impact of the R_w variability is low and particularly on the airflow resistivity parameter. It is interesting to note that the reticulation rate R_w explains almost 50 % of the sensitivity on the viscous characteristic length Λ even if the material only contains a maximum of 20 % of closed pores. This is in good agreement with the

definition of Λ for which the dependence to local particle velocity makes it more sensitive to the smaller constrictions within the bulk material; constrictions which are created by the presence of the membranes.

This analysis is confirmed when the sound absorption coefficient is considered. Figure 2(b) shows the sensitivity index SI of the three microstructure parameters on the sound absorption coefficient according to frequency (dashed color lines), the mean value of sound absorption coefficient (solid black line), together with its extrema (its minimum and maximum values which delimit the gray area), and also the mean value plus or minus the standard deviation (dotted black line) which can be considered as a global measure of total sensitivity. It is shown that strut length l of highly reticulated PU foams has the major impact on the sound absorption coefficient for almost all frequencies (see dashed green curve). It is also shown that the impact of the R_w parameter on the sound absorption coefficient is significant in the whole frequency range and even dominates at high frequencies (for $f >$ 3.6 kHz). This may indicate a dominant contribution of Λ and α_∞ (see Fig. 2(b)) in this frequency range since the viscous transition occurs at f_v =500 Hz. It is worth mentioning that the sound absorption coefficient variability (i.e., surface between the two dashed black lines) is moderate and can be considered acceptable. This indicates that the variability on both strut length and reticulation rate should not exceed 10 % as far as possible.

In the case of the poorly reticulated foam V2 (R_w = 20 %), Figs. 2(c) and 2(d) show that the reticulation rate is the most influent parameter and its impact on non-acoustic and acoustic properties is more pronounced. Indeed, the airflow resistivity is again the most impacted parameter and its NSD almost reaches 50 %. R_w explains the larger part of the variability of σ, Λ and α_∞ (see Fig. 2(c)). The strut length parameter l has a noticeable influence on both σ and Λ' but its influence on the sound absorption coefficient is poor

in the whole frequency range except at low frequencies around 500 Hz (see Fig. 2(d)). According to Figs. 2(c) and 2(d), it can be concluded that the thermal characteristic length Λ' has no influence on the absorption coefficient for this class of poorly reticulated materials; i.e., thermal effects are negligible compared to the viscous ones. This analysis is confirmed by the viscous transition frequency located at 2010 Hz indicating that the viscous effects are strong in the whole frequency range of interest. The strut length variability mainly impacts the sound absorption coefficient at low frequencies through the airflow resistivity parameter. The large variability observed for the airflow resistivity due to both R_w and l is thus responsible for the sound absorption variability which is particularly pronounced around the first sound absorption pick (i.e., 800 Hz). This analysis indicates that, in the case of poorly reticulated foams, the reticulation rate measurements should be performed with great care and should not be subjected to large inhomogeneity. The influence of the strut length variability is less important and is restricted to low frequencies (i.e., before the first sound absorption peak); this parameter can be subjected to bulk inhomogeneity and/or measured in a less precise manner.

Finally, considering now foam V3 with the large cells and moderate reticulation rate (C_s = 1 mm and R_w = 50 %), Fig. 2(e) shows that the output variability is moderate ($NSD < 30$ %). As for foam V1, most of the sensitivity on σ and Λ' is due to strut length l whereas most of the sensitivity on α_∞ and Λ is due to reticulation rate R_w. However, unlike foam V1, Λ is almost only controlled by the reticulation rate R_w since the amount of closed pores (i.e., 1-R_w) has been increased from 20% to 50%. According to Fig. 2(f), the reticulation rate R_w is preponderant in the frequency bands around the two picks of the sound absorption curve (here around 1 kHz and 3.5 kHz for the chosen sample thickness); while between these two picks, the strut length parameter l governs the sound absorption

variability. The viscous transition frequency being equal to 256 Hz for this material, Figs. 2(e) and 2(f) may indicate a stronger influence of the airflow resistivity for f <1500 Hz and a dominant viscous characteristic length and tortuosity for $f > 2500$ Hz. However, it is not straightforward from Fig. 2 to determine for each material the frequency bands where specific non-acoustic parameters are predominant because : (i) almost all non-acoustic properties are sensitive to R_w and l and (ii) the two transition frequencies f_v and f_t are located in the frequency range of interest meaning that the viscous, thermal and inertial interactions contribute to the foam acoustical behavior. The reader who wants to better assess the frequency bands where the macroscopic non-acoustic parameters contribute the most to the sound absorption behavior could refer to the previous work of Ouisse *et al.*[27].

As far as foams V1, V2 and V3 are concerned, Fig. 2 show that the influence of the strut thickness parameter t is low for the three virtual materials: a precision of 10 % has low impact on the output variability. Thus, a precise measurement of this microstructure parameter is not required. Conversely, strut length l and/or reticulation rate R_w variability is shown to clearly impact the non-acoustic parameters and particularly the airflow resistivity. However, it is worth keeping in mind that the microstructure variability was set to 10% and led to an acceptable global variability on the estimated sound absorption coefficient (see gray surface delimited by the mean value plus or minus the standard deviation). Thus, both microstructural parameters should be measured precisely and the materials of interest should exhibit moderate bulk inhomogeneity or natural cell anisotropy in order to keep a global variability within the range of 10%.

FIG. 2.

The sensitivity analysis is now applied to the 2-parameter semi-empirical model. The results presented in Figs. 3 indicate that all conclusions drawn previously on l and R_w for

the 3-parameter model sensitivity analysis can be transposed to C_s and R_w; i.e., both C_s and R_w contribute significantly to the outputs variability with a relative importance depending on the type of material. However, the variability of the 5 non-acoustic parameters and the sound absorption coefficient are less impacted by the cell size C_s variability associated to the 2-parameter model than the strut length l variability associated to the 3-parameter model. For example, the NSD of airflow resistivity σ in the case of the fully reticulated material V1 decreases from 27 % in the case of the 3-parameter model to almost 14 % in the case of the 2-parameter model (compare Figs. 2(a) and 3(a)). Indeed, a closer look at Eqs. (9) and (14) clearly indicates that the airflow resistivity is a function of l^4 in the 3-parameter model and a function of C_s^2 in the 2-parameter model. This favors the use of the 2-parameter model. However, this conclusion will be revisited in the following section since the effect of foam irregularities, foam inhomogeneity, natural anisotropy and uncertainties due to measurement procedures will be included in the analysis and will impact differently l and C_s.

FIG. 3.

It is worth mentioning that a sensitivity analysis has been first applied on the full set of PU foams (i.e., 500 $\mu m \leq C_s \leq 1500$ μm and 5 % $\leq R_w \leq$ 100 %) using the 2-parameter model. This analysis has not been presented here for conciseness. Because the two geometric factors A and B are given within a statistical range of variation, the 2-parameter model was first considered as a 4-parameter model from a statistical point of view. It was observed that A and B had almost no impact on the sensitivity of the 5 non-acoustic parameters and the sound absorption coefficient. This is mostly due to the fact that the model is restricted to porous foams for which the open porosity slightly varies. The 2-parameter model considering constant values for A and B is thus relevant.

B. Focus on sensitivity analysis of real foams M10, P1, P2 and P3

The sensitivity analysis is now applied to four real foams provided by the Woodbridge Group©. The microstructure of these foams is characterized following the process described in section II A. Foam P1 is a fully reticulated foam with a small cell size ($C_s = 673\ \mu m$). Materials M10 and P2 are partially reticulated foams with a small cell size ($C_s \approx 650\ \mu m$) and a moderate and low reticulation rate, respectively ($R_w \approx 70$ % for M10 and $R_w \approx 30$ % for P2). Finally, foam P3 is partially reticulated with a very large cell size ($C_s \approx 1700\ \mu m$) and a very low reticulation rate ($R_w = 5\%$). It is worth mentioning that an anisotropy has been observed for the reticulation rate parameter of material P3: i.e., a reticulation rate of 5 % is observed in the longitudinal direction (SEM pictures taken in the plane perpendicular to the wave propagation) and of 35 % in the transverse direction (SEM pictures taken in the plane parallel to the wave propagation). Only the coefficient measured in the plane perpendicular to the wave propagation is considered since it is the one that mainly impacts the wave propagation (the value of 5 % has been validated in ref.[8] when comparing sound absorption measurements and micro-macro predictions). Note that these four foams have already been presented in references[7,8] and are at the limits of the range of microstructure properties used in the first characterization set (i.e., for materials M1 to M15, $500\ \mu m < C_s < 1600\ \mu m$ and $10\% < R_w < 100\%$). All foams are considered quasi-isotropic with a $DA < 1.25$. The measured non-acoustic properties of the foams are given in Table II. Their microstucture properties are summarized in Table III. Mean values are provided together with the uncertainties levels which are related to measurement, anisotropy and heterogeneity of the sample. In coherence with the previous section dealing with virtual foams, the standard deviation for the three microstructure properties C_s, l and t is given as

a percentage of the mean value. Table III indicates that, the variability measured on strut dimensions is larger than the one measured on cell size and reticulation rate: the variability on C_s and R_w is globally below the threshold of 10 % (except for foam P3) and conversely, the variability on strut dimensions l and t slightly exceeds 10 %. For material P3, the larger variability on cell size can be attributed to the cell anisotropy which is at the limit of the threshold set to 1.25. The sensitivity analysis is applied for the 4 foams and to the 2 micro-macro based models. Strut dimensions and cell size are described by Gamma probability density functions identified from maximum-likelihood estimation using the large set of local measurements available on the various foam samples[27]. Concerning the reticulation rate, the low coupling effects associated to small amount of measurements and unclear physical limits of R_w on the samples of interest led us to use uniform probability density functions for this variable. The reason for this small amount of data is that the reticulation rate is estimated at a higher scale from the SEM pictures (i.e., meso-scale, see Sec. II A). A deeper analysis of the impact of the choice of probability density functions, can be found in reference[27].

All real materials are 1 in. thick, except for material M10 which is 2 in. thick. The results of the sensitivity analysis are given in Figs. 4-7.

FIG. 4.

FIG. 5.

FIG. 6.

FIG. 7.

The reticulation rate of foam P1 is 100%, hence tortuosity is constant and its normalized standard deviation is null as shown in Fig. 4(a). The porosity is barely affected by the

measured variability on l and t and its NSD is close to 0. For the other non-acoustical parameters (σ, Λ and Λ'), the trends are equivalent, namely more than 3/4 of the sensitivity is due to the strut length l while less than 1/4 is due to strut thickness t. The NSD of these non-acoustical parameters is high, particularly for the airflow resistivity. As far as the acoustic features are concerned (see Fig. 4(b)), relative contributions are consistent with the observations made on non-acoustic parameters: the fully reticulated foam P1 exhibits almost constant sensitivity indexes on the frequency range of interest, confirming the fact that the strut length l has much more impact on the variations of the outputs than the strut thickness t. The sound absorption coefficient derived from the 3-parameter model is underestimated compared to impedance tube measurements because the airflow resistivity is underestimated. This fact is already commented in details in reference[8]. The sensitivity analysis mainly shows that the strut length parameter is the key parameter for fully reticulated materials since it greatly impacts three important non-acoustic parameters. However, it also induces large uncertainty on the sound absorption coefficient as shown in Fig. 4(b) even if its measurement variability is moderate (i.e., the standard deviation is less than 15% of the mean value). This parameter should be measured with great care and only fully isotropic foams should be considered with a DA as close as possible of 1 in order to minimize the strut length variability. The sensitivity analysis applied to the 2-parameter model (see Figs. 4(c) and 4(d)) shows that both the non-acoustic parameters and the sound absorption coefficient are less impacted by the cell size variability. Indeed, as mentioned in the case of the virtual foams, the 2-parameter model is less impacted by the cell size variability than the 3-parameter model by the strut length variability. Furthermore, as far as foam P1 is concerned, the measurement variability on cell size is less important than the one of the strut length. This tends to promote the 2-parameter model. Indeed, the variability

on the estimated sound absorption is reduced (see Fig. 4(d)) and the agreement between sound absorption measurements and estimates is improved. However, the model still shows differences compared to measurements since the simple expression Eq.(14) underestimates the airflow resistivity for material P1[8] (σ is measured at 3490 N.s.m^{-4} and estimated from Eq.(14) at 2760 N.s.m^{-4}).

Consider now the two partially reticulated foams M10 and P2 which sensitivity analysis are presented in Figs. 5 and 6 respectively. These two foams share identical microstructure properties both in terms of mean values and standard deviations. The main difference is the amount of open pores; the foam M10 is moderately reticulated with $R_w = 69\%$ and the foam P2 is poorly reticulated with $R_w = 32\%$. However, the expanded uncertainty on R_w measured for both foams is identical and close to 10%. The two materials also slighlty differ by their strut variability; material M10 shows larger variability (i.e., 13 % of the mean value for M10 and 10 % for P2). Furthermore, the sample of material M10 is 2 in. thick whereas the sample of material P2 is 1 in. thick.

For both foams, the sensitivity analysis applied to the 3-parameter model indicates that, once again, the impact of the strut length parameter is important on the three non-acoustic parameters σ, Λ and Λ' (see Figs. 5(a) and 6(a)); the most impacted parameter with the greater NSD being the airflow resistivity σ. Except for the tortuosity, the variability on all non-acoustic parameters (i.e., NSD) is greater in the case of material M10 compared to material P2 most likely due to the larger strut length variability measured for M10. The sound absorption variability of material M10 is thus more important as shown in Figs. 5(b) and 6(b). Indeed, Fig. 5(b) shows that the strut length is the most sensitive parameter on the whole frequency range. The impact of R_w increases logically with the amount of closed pores (see Figs. 5(a) and 6(a)); for example, the reticulation rate explains almost

25% of the sensitivity on the viscous characteristic length Λ for material M10 and 65% for material P2. It also explains 3% of the sensitivity on the airflow resistivity σ for material M10 and 16% for material P2. For both cases, the reticulation rate captures all sensitivity effects on tortuosity α_∞ and the strut length explains almost 90% of the sensitivity on the thermal characteristic length Λ'. Fig. 6(b) indicates that the effect of R_w on the sound absorption coefficient of material P2 is predominant but the impact of the strut length l is non negligible. l even dominates around the first dip in the sound absorption curve, i.e. around 4 kHz in this case considering the given thickness of 1 inch. l also dominates at very low frequencies ($f < 100$ Hz) but it is not relevant since the variability of the sound absorption is null in this frequency range. This is coherent with the known effect of Λ' on α curves documented in the literature[27,28].

The sensitivity analysis applied to the 2-parameter model (see Figs. 5(c), 5(d), 6(c) and 6(d)) confirms that both the non-acoustic parameters and the sound absorption coefficient are less impacted by the cell size variability. In the case of foam P2, the variability on l and C_s is identical and close to 10% of the mean value; the improvement is thus only due to the low sensitivity of the 2-parameter model to C_s, as discussed in sec. IV A (i.e., the airflow resistivity in the 2-parameter model is a function of C_s^2). As far as foam M10 is concerned, the cell size variability is also reduced compared to strut length variability as indicated in Table III. The reticulation rate R_w thus becomes the most sensitive parameter for all non-acoustic and acoustic properties as presented in Figs. 5(c) and 5(d). The NSD of all non-acoustic properties are also greatly reduced so as the variability on the sound absorption coefficient.

The impact of the thickness of the samples on the results is obvious: we recall that the thickness of samples P1-P3 is 1 inch while the thickness of the sample M10 and the virtual

samples V1-V3 is 2 inches. By comparing the results obtained on P2 and M10 on one side and V2 on the other side, it can clearly be seen that a change in the thickness of the sample has a homothetic effect on the frequency effects. This point is justified by the fact that a rigid frame model has been used in this work.

Finally, the sensitivity analysis is applied to the poorly reticulated foam P3 characterized by a very large cell size, a very low reticulation rate $R_w = 5\% \pm 4\%$. The measured uncertainty on R_w is important in comparison with the mean value. The results of the sensitivity analysis is presented in Fig. 7. The airflow resistivity σ, the tortuosity α_∞ and the viscous length Λ greatly vary with input parameters, and their values are mainly driven by the reticulation rate R_w. The NSD of these non-acoustical parameters is very high, particularly for the airflow resistivity. The strut length parameter has a noticeable influence on both σ and Λ' but in this case, its influence on the sound absorption coefficient is poor in the whole frequency range (see Fig. 7(b)). It can be concluded that the thermal characteristic length Λ' has no influence for this class of material; i.e., thermal effects are negligible compared to the viscous ones. The low thermal transition frequency (i.e., 128 Hz) and the high viscous transition frequency (i.e., 1142 Hz) confirm this analysis. The sound absorption variability is very high in this case (see gray area between back dashed curves in Figs. 7(b) and 7(d)). However, it is considered acceptable since it includes measured values which are themselves highly impacted by variability due to frame vibration and sample lateral boundary conditions inside the impedance tube. The sensitivity analysis carried out on foam P3 is in good agreement with the one carried out on the virtual foam V2. In this case, only the reticulation rate R_w should be identified in a precise manner.

V. COMMENTS ON INVERSE MODELS

Due to the great complexity of characterizing precisely the PUC properties of such disordered network that constitutes the PU porous frame (particularly l and R_w), microstructure-based models can be used in an inverse procedure to get input equivalent microstructure properties from measurement of macroscopic parameters[10] (e.g., porosity ϕ, airflow resistivity σ). The foam under investigation should of course respect the main assumptions of the model. The objective of this section is to use the conclusions derived from the presented sensitivity analysis in order to investigate the relevance of using the 3-parameter and 2-parameter semi-empirical models in an inverse approach. Two main questions arise. Which macroscopic parameter should be considered preferentially as input to the inverse approach depending on the microstructural parameter of interest? and more specifically, should a macroscopic parameter impacted by at least two microstructure parameters be used in an inverse approach? To answer the first question, a macroscopic parameter that (i) depends only on one microstructural variable and (ii) is highly sensitive to this microstructure property (i.e., show a high NSD) is obviously the most relevant. Only the tortuosity is concerned here since it depends only on R_w according to Eq. (11). However, this property is not commonly measured and can be subjected to high measurement variability; α_∞ is thus not the most relevant parameter to get R_w and particularly for high values of α_∞. The sensitivity analysis shown that the airflow resistivity is usually the most sensitive output parameter. It is thus a good candidate for assessing the reticulation rate R_w from inverse method. However it is impacted by both the strut length l and the reticulation rate R_w. Determining R_w from σ thus requires that (i) the strut length parameter is not subjected to large variability and (ii) it is measured precisely. This is clearly a critical point since it

has been shown in this paper that this parameter, as it is measured, can show an important measurement variability. This is observed particularly when $R_w > 50\%$ as for foams V3 and M10. Indeed, for these two foams, Figs. 2(e) and 5(a) show that σ is poorly impacted by R_w but mainly by l. Once again, this favors the use of a model that depends on C_s and not on l to get R_w from σ; i.e. the 2-parameter model.

VI. CONCLUSION

This paper investigated the impact of polyurethane foam microstructure irregularity on the estimation of their macroscopic acoustic ($\alpha(\omega)$) and non-acoustic properties (σ, α_∞,...) using a robust sensitivity analysis performed on two semi-empirical unit-cell models. In these models, the porous material is idealized as a packing of an isotropic tetrakaidecahedra PUC representative of the disordered network that constitutes the porous frame. The PUC microstructure properties are measured directly from SEM micrographs. The main sources of measurement uncertainty on the PUC properties are related to bulk inhomogeneity, microstructural irregularities, natural anisotropy and limitations of the used measurement methods. The sensitivity analysis shows that, depending on the PUC microstructure parameter, the measured variability (due to natural cell anisotropy, inhomogeneity within the bulk volume and measurement bias) may have a significant influence on the model output variability. When the 3-parameter model is considered, all the analyses made on virtual and real foams show that the impact of measurement variability on strut thickness t is low. Thus, a precise measurement of this microstructure parameter is not required. For moderately and highly reticulated foams (i.e., $R_w > 30\%$), the sensitivity analysis mainly shows that the strut length parameter l is the key parameter since it greatly impacts three important non-acoustic parameters (σ, Λ and Λ'). It also causes large uncertainty on the

sound absorption coefficient even if its measurement variability is moderate (e.g., foams P1 and M10). This parameter should be measured with great care and only fully isotropic foams should be considered with a DA as close as possible of 1 in order to minimize the microstructure variability. For this class of PU foam, the impact of R_w variability is low and it can be identified in a less precise manner. In the case of poorly reticulated PU foams (i.e., $R_w < 30\%$), it is concluded that only the reticulation rate R_w should be identified in a precise manner. Indeed, it explains the larger part of the high variability observed of σ, Λ and α_∞ and controls the sound absorption coefficient in the whole frequency range.

For foams with a slight inhomogeneity and anisotropy, the 2-parameter model associated to cell size measurement should be preferred since (i) this model is less affected by cell size variability and (ii) it has been observed that for this type of foams, the cell size measurement is less impacted by bulk variability than the strut length parameter.

ACKNOWLEDGMENTS

The authors would like to thank the National Sciences and Engineering Research Council of Canada (NSERC) for providing financial support. This work was co-financed by The French National Research Agency under grant ANR-12-JS09-008-COVIA.

REFERENCES

[1]J.-L. Auriault, C. Boutin, and C. Geindrau. *Homogenization of coupled phenomena in heterogeneous media*. (ISTE, Hoboken, USA and Wiley, London, UK), 2009. Chap. 3, pp. 75-106 and Chap. 7, pp. 197-226.

[2]D. L. Johnson, J. Koplik, and R. Dashen. Theory of dynamic permeability and tortuosity in fluid-saturated porous media. *Journal of Fluid Mechanics*, 176:379–402, 1987.

[3]Y. Champoux and J. F. Allard. Dynamic tortuosity and bulk modulus in air-saturated porous media. *Journal of applied physics*, 70(4):1975–1979, 1991.

[4]J. F. Allard and N. Atalla. *Propagation of sound in porous media: modelling sound absorbing materials*. (Wiley, Chichester, UK), 2nd edition, 2009. Chap. 4, pp. 45-72 and Chap. 5, pp. 73-107.

[5]J.L Gibson and M.F. Ashby. *Cellular Solids-Structure and Properties*. (Cambridge University Press, Cambridge, USA), 1997. 532 pp.

[6]A. Cummings and S. P. Beadle. Acoustic properties of reticulated plastic. *Journal of Sound and Vibration*, 175(1):115–133, 1993.

[7]O. Doutres, N. Atalla, and K. Dong. Effect of the microstructure closed pore content on the acoustic behavior of polyurethane foams. *Journal of Applied Physics*, 110(6):064901, 2011.

[8]O. Doutres, N. Atalla, and K. Dong. A semi-phenomenological model to predict the acoustic behavior of fully and partially reticulated polyurethane foams. *Journal of Applied Physics*, 113(5):054901, 2013.

[9]C. Perrot, F. Chevillotte, M.T. Hoang, G. Bonnet, and F.X. Becot. Microstructure, transport, and acoustic properties of open-cell foam samples: Experiments and three-dimensional numerical simulations. *Journal of Applied Physics*, 111:014911, 2012.

[10]M.T. Hoang and C. Perrot. Solid films and transports in cellular foams. *Journal of Applied Physics*, 112:054911, 2012.

[11]F. Chevillotte, C. Perrot, and E. Guillon. A direct link between microstructure and acoustical macro-behavior of real double porosity foams. *Journal of the Acoustical Society*

of America, 134(6):4681–4690, 2013.

[12]H.X. Zhu, J.F. Knott, and N.J. Mills. Analysis of the elastic properties of open-cell foams with tetrakaidecahedral cells. *J. Mech. Phys. Solids*, 45(3):319–343, 1997.

[13]L. Gong, S. Kyriakides, and Jang W.-Y. Compressive response of open-cell foams. part i: Morphology and elastic properties. *International Journal of Solids and Structures*, (42):13551379, 2005.

[14]H.X. Zhu, J.R. Hobdell, and A.H. Windle. Effect of cell irregularity on the elastic properties of open-cell foams. *Acta mater.*, 48:4893–4900, 2000.

[15]A. Saltelli, K. Chan, and E. M. Scott. *Sensitivity analysis*. (Wiley, New York, USA), 2000. 504 pp.

[16]R. I. Cukier, C. M. Fortuin, K. E. Shuler, A .G. Petschek, and J. H. Schaibly. Study of the sensitivity of coupled reaction systems to uncertainties in rate coefficients. I Theory. *The Journal of Chemical Physics*, 59:3873, 1973.

[17]J. H. Schaibly and K. E. Shuler. Study of the sensitivity of coupled reaction systems to uncertainties in rate coefficients. II Applications. *The Journal of Chemical Physics*, 59:3879, 1973.

[18]R. I. Cukier, J. H. Schaibly, and K. E. Shuler. Study of the sensitivity of coupled reaction systems to uncertainties in rate coefficients. III. Analysis of the approximations. *The Journal of Chemical Physics*, 63:1140, 1975.

[19]W.E. Lox and W. Petrich. Reticulated polyurethane foam and method of making same, 1973. US Patent 3,753,756.

[20]Caroline A Schneider, Wayne S Rasband, and Kevin W Eliceiri. Nih image to imagej: 25 years of image analysis. *Nat Methods*, 9(7):671–675, 2012.

[21]P. Göransson, R. Guastavino, and N.E. Hörlin. Measurement and inverse estimation

of 3d anisotropic flow resistivity for porous materials. *Journal of Sound and Vibration*, 327:354367, 2009.

[22]C. Zhang, J. J. Li, Z. Hu, F. Zhu, , and Y. Huang. Correlation between the acoustic and porous cell morphology of polyurethane foam: Effect of interconnected porosity. *Materials and Design*, 41:319–325, 2012.

[23]E. Lind-Nordgren and P. Göransson. Optimising open porous foam for acoustical and vibrational performance. *Journal of Sound and Vibration*, 329:753–767, 2010.

[24]Anonymous. Standard test method for flexible cellular materials slab, bonded, and molded urethane foams. *American Society for Testing and Materials ASTM D3574*.

[25]I. M. Sobol. Global sensitivity indices for nonlinear mathematical models and their Monte Carlo estimates. *Mathematics and Computers in Simulation*, 55(1-3):271–280, 2001.

[26]A. Saltelli, S. Tarantola, and K. P. S. Chan. A quantitative model-independent method for global sensitivity analysis of model output. *Technometrics*, 41(1):39–56, 1999.

[27]M. Ouisse, M. Ichchou, S. Chedly, and M. Collet. On the sensitivity analysis of porous material models. *Journal of Sound and Vibration*, 331(24):52925308, 2012.

[28]Y. Atalla and R. Panneton. Inverse acoustical characterization of open cell porous media using impedance tube measurements. *Canadian Acoustics*, 33(1):11–24, 2005.

TABLE I. Microstructure properties of the three virtual foams.

Material	C_s μm nominal	C_s μm (min,max)	R_w % nominal	R_w % (min,max)
V1	500	(450, 550)	80	(70, 90)
V2	500	(450, 550)	20	(10, 30)
V3	1000	(900, 1100)	50	(40, 60)

TABLE II. Non-acoustic properties of the foams and transition frequencies.

Material	ϕ (%)	σ (N.s.m^{-4})	α_∞	Λ (μm)	Λ' (μm)	f_v (Hz)	f_t (Hz)
V1	98.4	6 410	1.14	128	232	724	500
V2	98.4	30 130	1.93	31	142	2 010	1 330
V3	98.4	2 710	1.36	142	353	256	216
P1	95.6	3 490	1.06	187	250	412	433
M10	98.2	3 670	1.25	240	310	378	280
P2	95.8	17 440	1.73	46	220	1 267	557
P3	97.1	19 360	2.16	24	458	1 142	128

TABLE III. Microstructure properties of the four real foams.

Material	C_s		l		t		R_w		Degree of anisotropy DA
	mean (μm)	Stdeva (% of mean)	mean (μm)	Stdeva (% of mean)	mean (μm)	Stdeva (% of mean)	mean (%)	expanded uncertainty (%)	
P1	673	9	208	14	53	14	100	-	1.12
M10	681	3	204	13	62	11	69	9	1.10
P2	637	9	213	10	58	9	32	9	1.14
P3	1751	15	554	12	172	10	5	4	1.25

Figure Captions

Figure 1. (a) shape of the periodic unit cell (PUC) for isotropic polyurethane foams; (b) cell size C_s measurements; (c) strut length l and strut edge a measurements; (d) reticulation rate R_w measurements.

Figure 2. Sensitivity analysis of the 3-parameter model for the three virtual foams V1, V2 and V3. First line: First-order sensitivity index SI for macroscopic non-acoustic parameters and associated Normalized Standard Deviation NSD. Second line: normal incidence sound absorption (bold line: mean value; dotted line: standard deviation; gray area: extremal bounds) and associated first-order sensitivity index SI. Viscous/inertial transition frequency f_v and isothermal/adiabatic transition frequency f_t are also shown on the plots.

Figure 3. Sensitivity analysis of the 2-parameter model for the three virtual foams V1, V2 and V3. First line: First-order sensitivity index SI for macroscopic non-acoustic parameters and associated Normalized Standard Deviation NSD. Second line: normal incidence sound absorption (bold line: mean value; dotted line: standard deviation; gray area: extremal bounds) and associated first-order sensitivity index SI. Viscous/inertial transition frequency f_v and isothermal/adiabatic transition frequency f_t are also shown on the plots.

Figure 4. Sensitivity analysis on the real foam P1. First line: First-order sensitivity index SI for macroscopic non-acoustic parameters and associated Normalized Standard Deviation NSD. Second line: normal incidence sound absorption (bold line: mean value; dotted line: standard deviation; gray area: extremal bounds) and associated first-order sensitivity index SI. Viscous/inertial transition frequency f_v and isothermal/adiabatic transition frequency f_t are also shown on the plots.

Figure 5. Sensitivity analysis on the real foam M10. First line: First-order sensitivity index

SI for macroscopic non-acoustic parameters and associated Normalized Standard Deviation NSD. Second line: normal incidence sound absorption (bold line: mean value; dotted line: standard deviation; gray area: extremal bounds) and associated first-order sensitivity index SI. Viscous/inertial transition frequency f_v and isothermal/adiabatic transition frequency f_t are also shown on the plots.

Figure 6. Sensitivity analysis on the real foam P2. First line: First-order sensitivity index SI for macroscopic non-acoustic parameters and associated Normalized Standard Deviation NSD. Second line: normal incidence sound absorption (bold line: mean value; dotted line: standard deviation; gray area: extremal bounds) and associated first-order sensitivity index SI. Viscous/inertial transition frequency f_v and isothermal/adiabatic transition frequency f_t are also shown on the plots.

Figure 7. Sensitivity analysis on the real foam P3. First line: First-order sensitivity index SI for macroscopic non-acoustic parameters and associated Normalized Standard Deviation NSD. Second line: normal incidence sound absorption (bold line: mean value; dotted line: standard deviation; gray area: extremal bounds) and associated first-order sensitivity index SI. Viscous/inertial transition frequency f_v and isothermal/adiabatic transition frequency f_t are also shown on the plots.

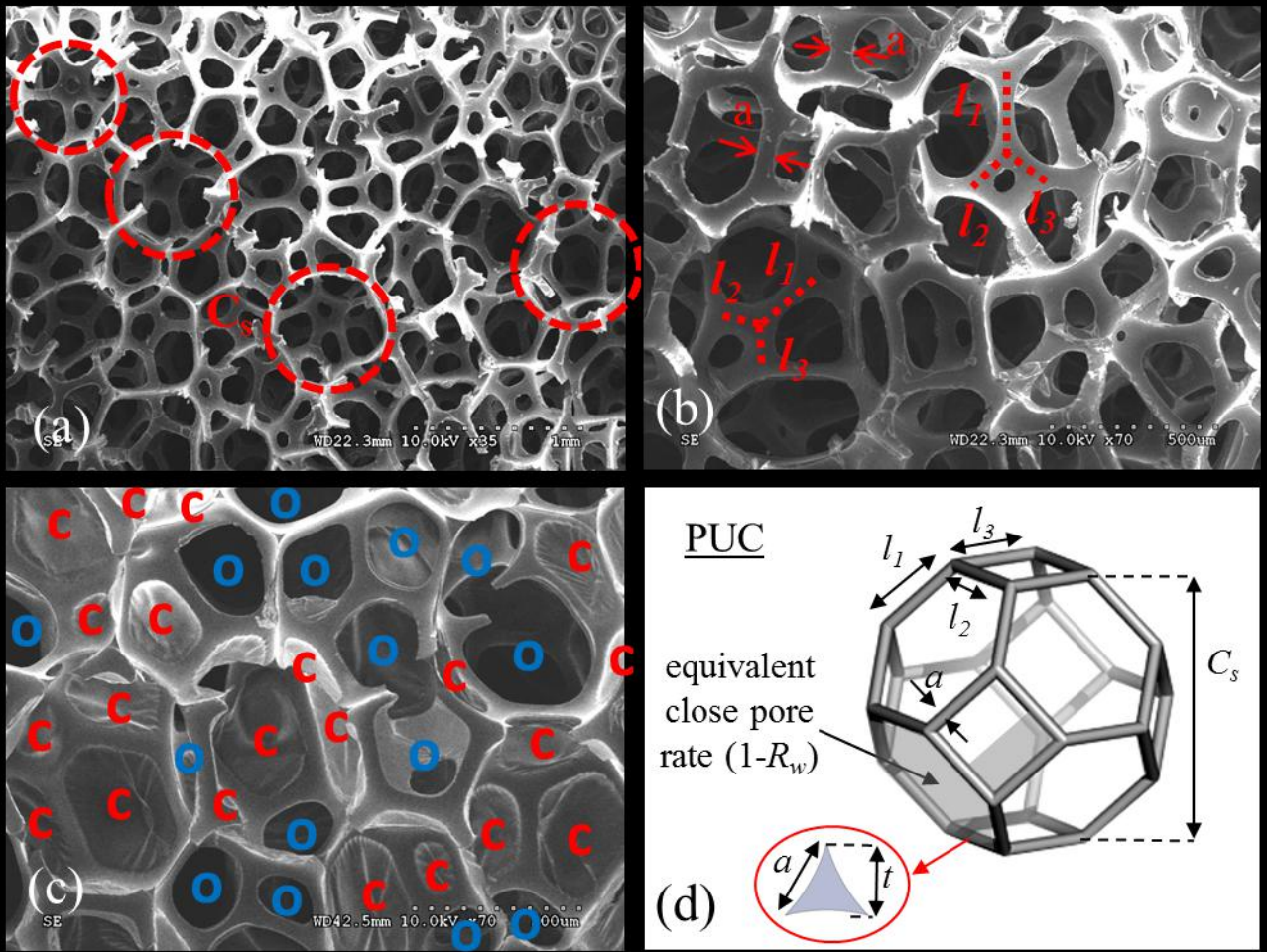
(a)
C_s
(b)
a
a
l_1
l_2
l_3
l_2
l_1
l_3
(c)
C
O
(d)
PUC
l_3
l_1
l_2
C_s
a
equivalent close pore rate (1-R_w)
a
t

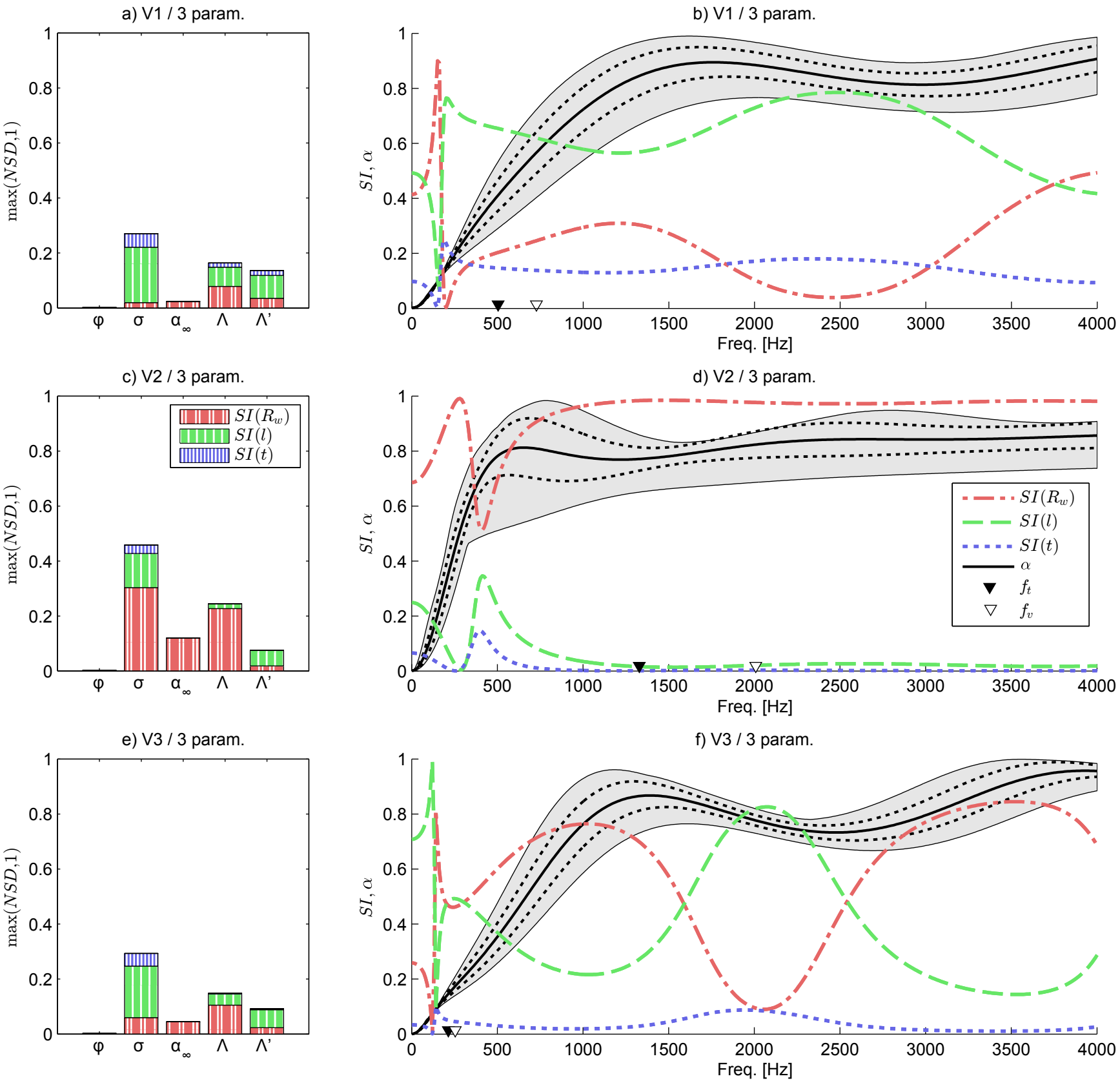
a) V1 / 3 param.
b) V1 / 3 param.
c) V2 / 3 param.
d) V2 / 3 param.
e) V3 / 3 param.
f) V3 / 3 param.
max(NSD,1)
SI, α
Freq. [Hz]
φ
σ
α∞
Λ
Λ'
SI(Rw)
SI(l)
SI(t)
α
ft
fv

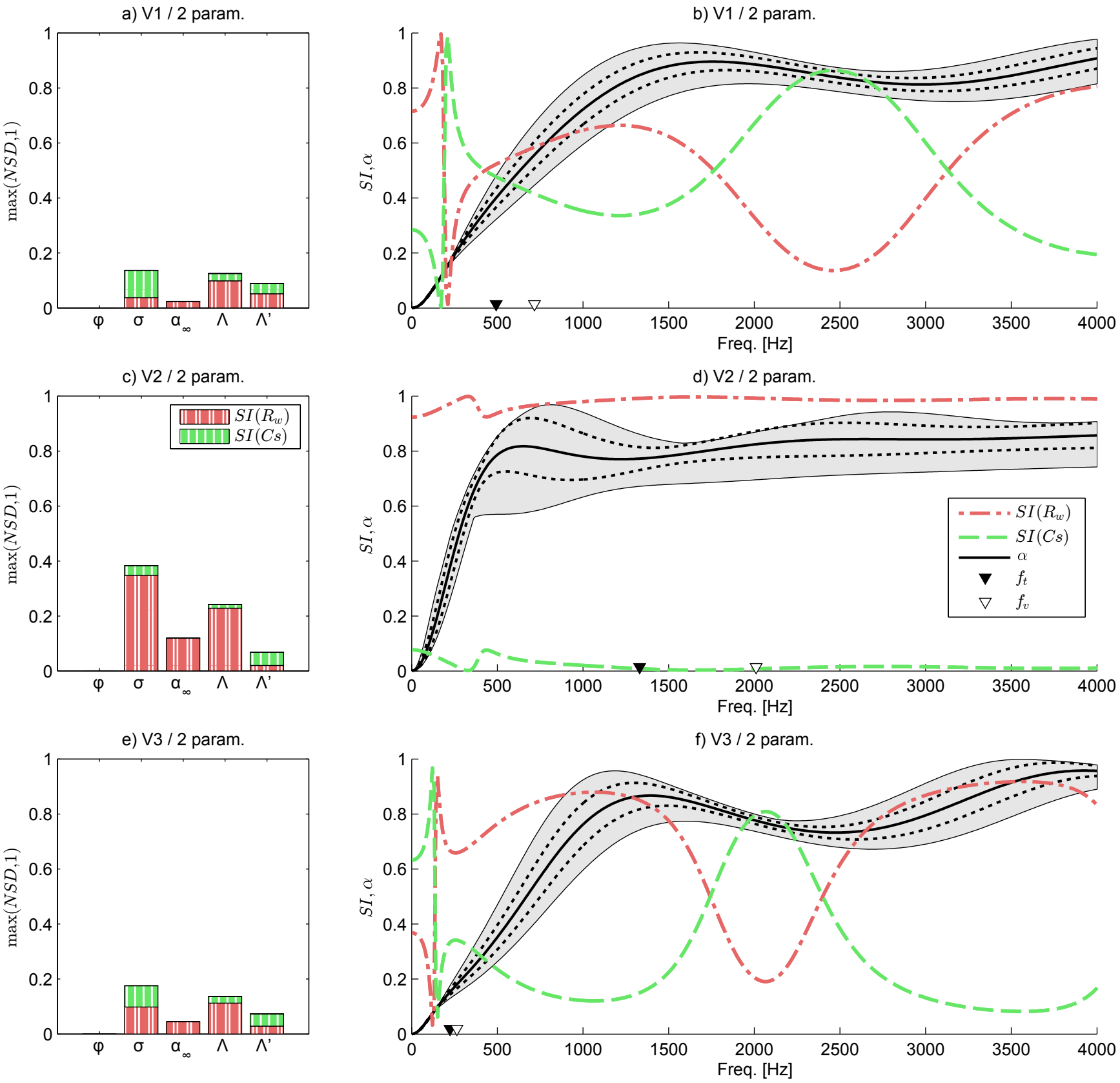
a) V1 / 2 param.
b) V1 / 2 param.
c) V2 / 2 param.
d) V2 / 2 param.
e) V3 / 2 param.
f) V3 / 2 param.
max(NSD,1)
SI, α
Freq. [Hz]
φ
σ
α∞
Λ
Λ'
SI(Rw)
SI(Cs)
α
ft
fv

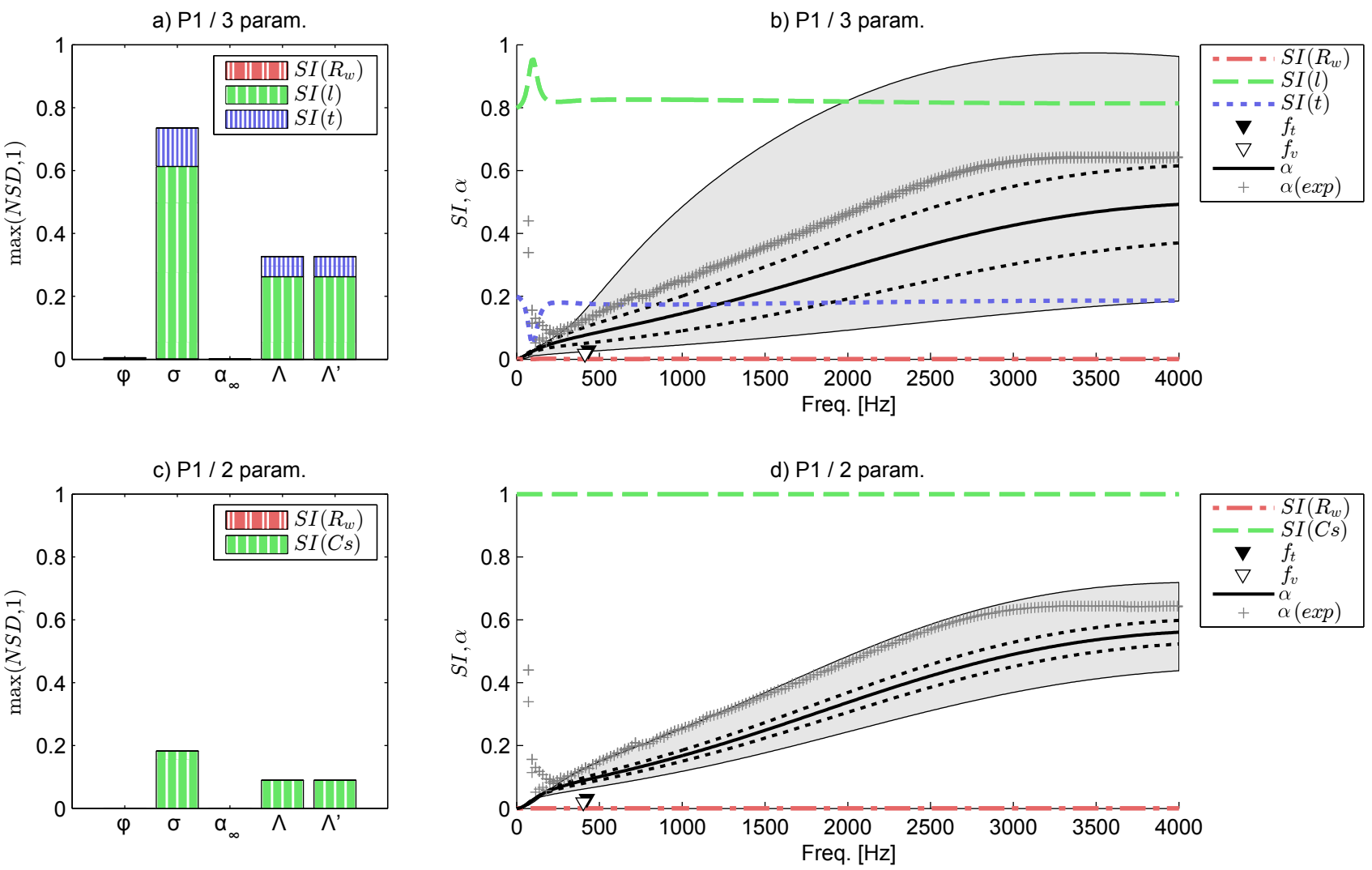
a) P1 / 3 param.
b) P1 / 3 param.
c) P1 / 2 param.
d) P1 / 2 param.
max(NSD,1)
SI, α
Freq. [Hz]
SI(Rw)
SI(l)
SI(t)
SI(Cs)
ft
fv
α
α(exp)
φ
σ
α∞
Λ
Λ'

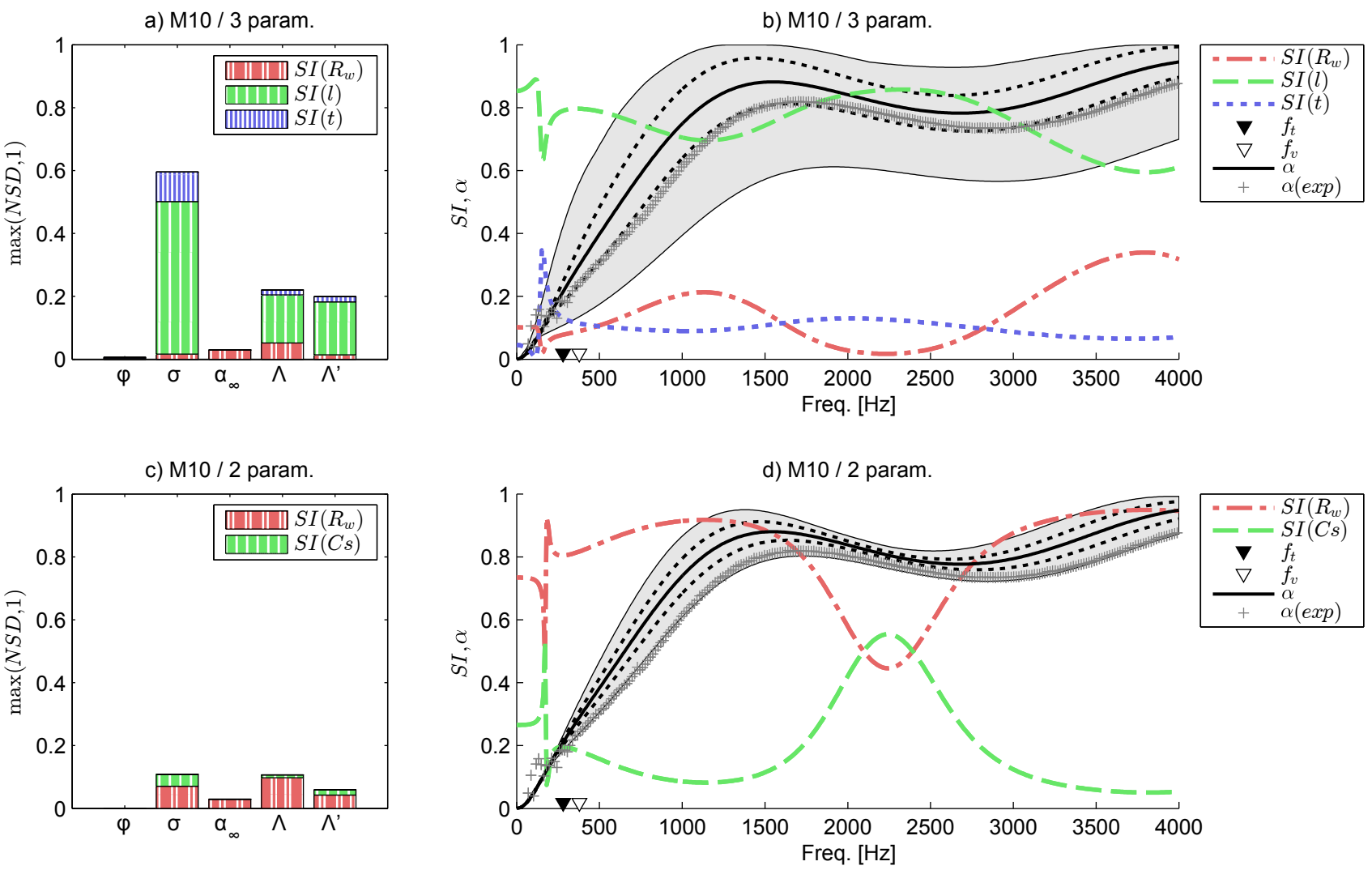
a) M10 / 3 param.
b) M10 / 3 param.
c) M10 / 2 param.
d) M10 / 2 param.
max(NSD,1)
SI, α
Freq. [Hz]
SI(R_w)
SI(l)
SI(t)
SI(Cs)
f_t
f_v
α
α(exp)
φ
σ
α_∞
Λ
Λ'

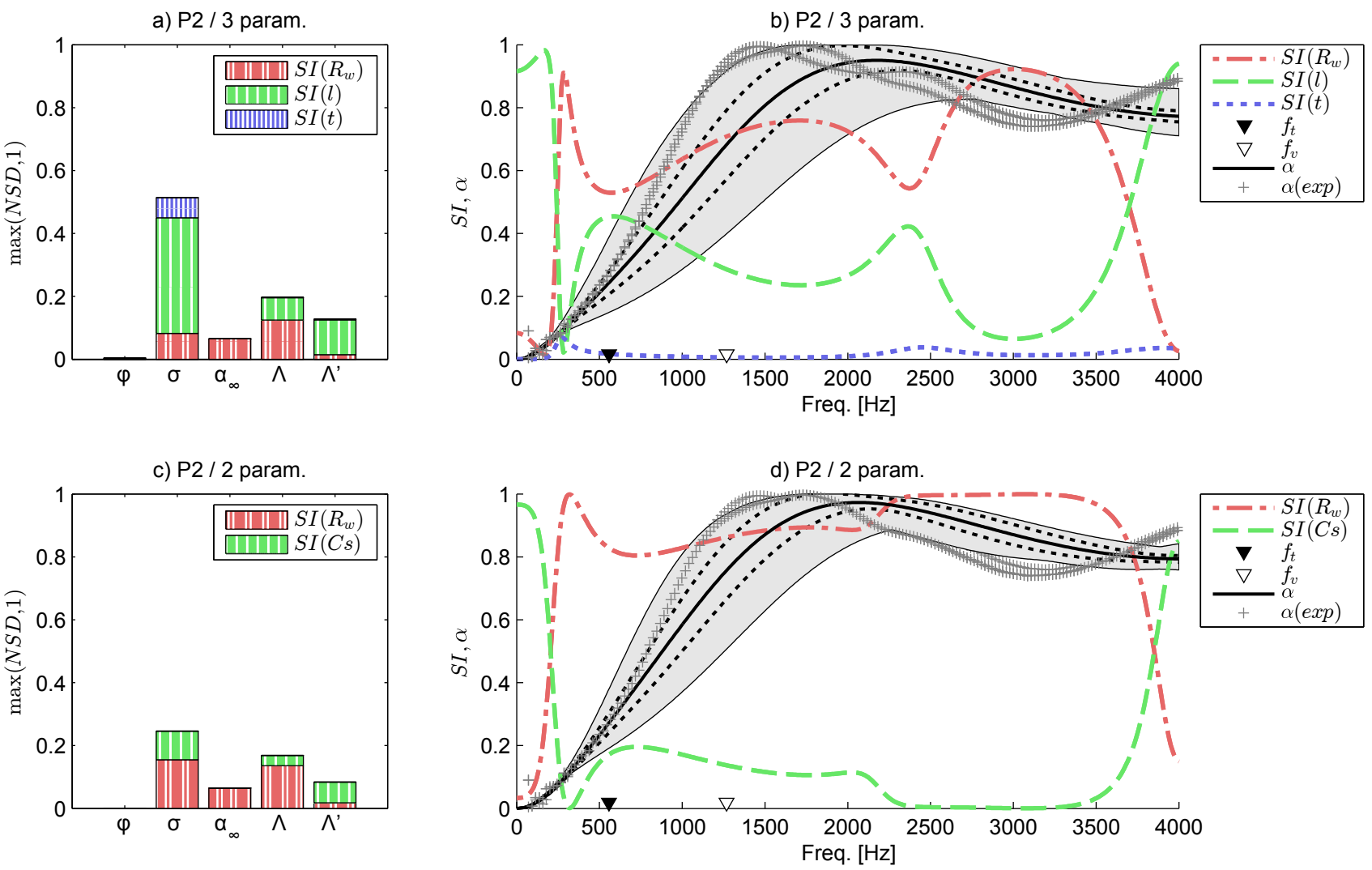
a) P2 / 3 param.
b) P2 / 3 param.
c) P2 / 2 param.
d) P2 / 2 param.
max(NSD,1)
SI, α
Freq. [Hz]
SI(Rw)
SI(l)
SI(t)
SI(Cs)
ft
fv
α
α(exp)
φ
σ
α∞
Λ
Λ'

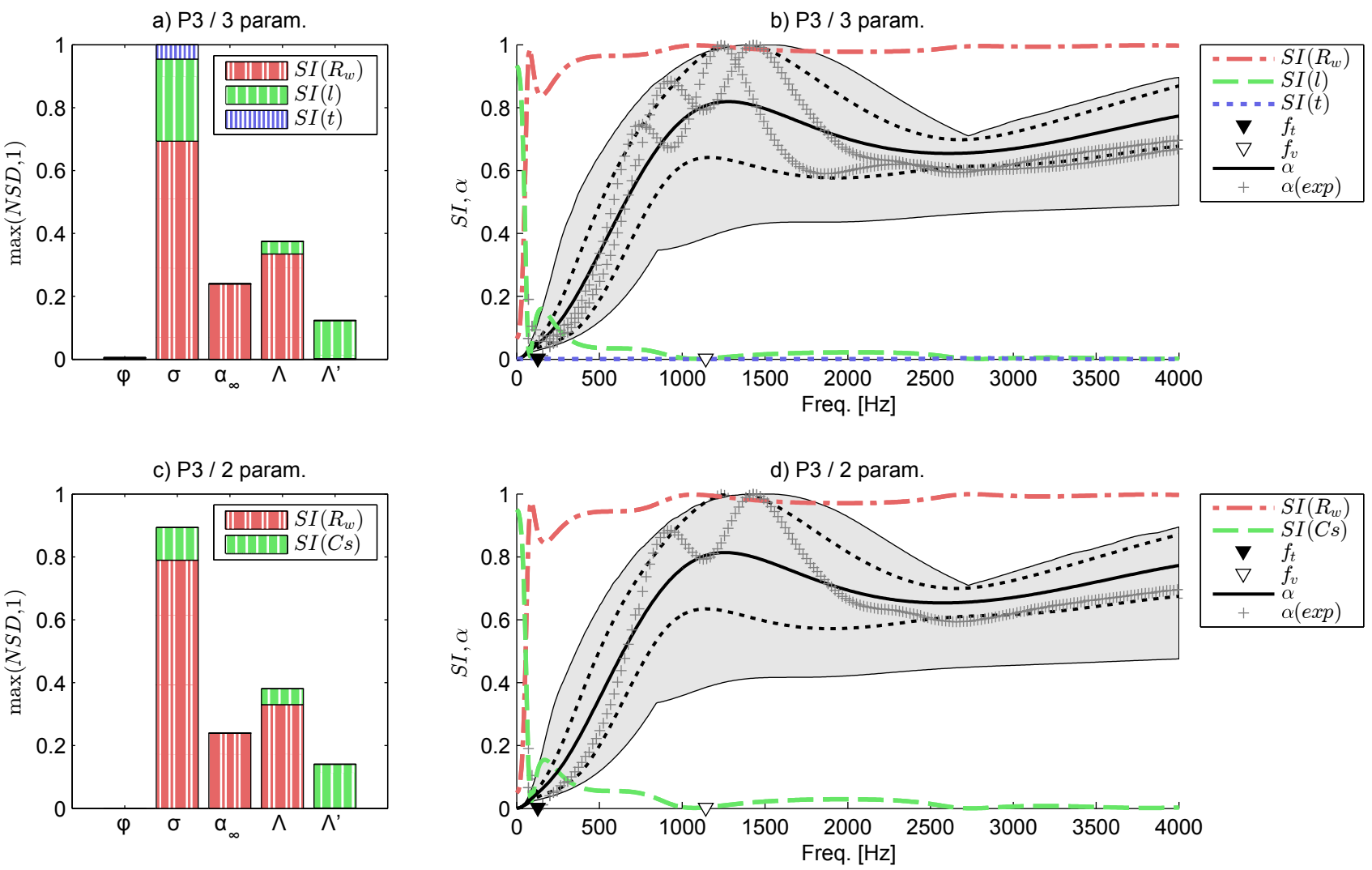
a) P3 / 3 param.
max(NSD,1)
SI(Rw)
SI(l)
SI(t)
φ
σ
α∞
Λ
Λ'
b) P3 / 3 param.
SI, α
Freq. [Hz]
SI(Rw)
SI(l)
SI(t)
ft
fv
α
α(exp)
c) P3 / 2 param.
max(NSD,1)
SI(Rw)
SI(Cs)
φ
σ
α∞
Λ
Λ'
d) P3 / 2 param.
SI, α
Freq. [Hz]
SI(Rw)
SI(Cs)
ft
fv
α
α(exp)